

Predicting the performance of tungsten in a fusion environment: a literature review

R.G. Abernethy

To cite this article: R.G. Abernethy (2017) Predicting the performance of tungsten in a fusion environment: a literature review, Materials Science and Technology, 33:4, 388-399, DOI: [10.1080/02670836.2016.1185260](https://doi.org/10.1080/02670836.2016.1185260)

To link to this article: <https://doi.org/10.1080/02670836.2016.1185260>



© 2016 The Author(s). Published by Informa UK Limited, trading as Taylor & Francis Group



Published online: 06 Jun 2016.



Submit your article to this journal [↗](#)



Article views: 1532



View Crossmark data [↗](#)



Citing articles: 8 View citing articles [↗](#)

Predicting the performance of tungsten in a fusion environment: a literature review

R.G. Abernethy* 

Tungsten has been proposed for use in the divertor of future fusion devices. In this environment, it will be exposed to high heat fluxes, neutron damage and hydrogen and helium implantation. This review covers previous experimental and modelling work to establish our ability to predict the performance of tungsten in a fusion environment. Surrogates for high-energy neutrons have been used to predict the change in mechanical properties of tungsten, including fission neutron and self-ion exposure. These studies are critically analysed, with a focus on the difference in results from neutron and ion studies. Further studies to improve our ability to predict the performance of tungsten are proposed as a critical part of the path towards a working fusion reactor.

Keywords: Tungsten, Rhenium, Neutron irradiation, Ion irradiation, Nanoindentation, Irradiation hardening, Fusion materials, Irradiation-induced precipitation

This review was submitted as part of the 2016 Materials Literature Review Prize of the Institute of Materials, Minerals and Mining run by the Editorial Board of MST. Sponsorship of the prize by TWI Ltd is gratefully acknowledged

Introduction

Fusion for energy

Human demand for electricity is increasing at a faster rate than ever before. Rapidly growing economies in the developing world combined with population growth results in a predicted 70% increase in electricity demand by 2040.¹ This increase in demand must be offset against the need to reduce carbon emissions from electricity production in order to avoid catastrophic climate change.²

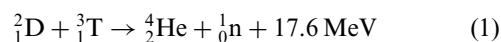
While extensive progress has been made in other carbon-free sources of electricity, such as solar or coal with carbon capture and storage, concerns over reliability of supply or cost means that nuclear energy is likely to become an increasingly important source of baseline electricity supply.³

Nuclear fission has been used extensively as a source of electricity since its advent in the 1950s, especially in countries such as France where 80% of electricity is generated by nuclear power plants. However, concerns over long-lived radioactive waste and public safety are resulting in increasing costs and political moves away from nuclear power, especially in wake of the Fukushima disaster in 2011.

Balancing the above factors is leading to a drive towards developing nuclear fusion into a viable source of electricity. Careful reactor design will allow fusion to be an efficient, affordable, low-carbon energy source with no long-lived radioactive waste and inherent safety.^{4,5} However, before a fusion power plant can be constructed, scientific advances are required in several areas including plasma physics and radiation-resistant materials capable of operating at high temperatures.⁶

Reactor design

The current leading design for a fusion reactor is the Tokamak. Tokamaks use a strong toroidal magnetic field to confine a plasma at 150 million K. At this temperature, deuterium and tritium ions can overcome electrostatic repulsion and fuse together releasing energy (see equation (1)).



Helium produced from the reaction must be extracted and other particles will also drift outside the confined plasma volume. These energetic particles pass through the last closed flux surface into the scrape-off layer. In this region, the ions will follow open flux lines until they collide with a surface (see Fig. 1). In large-scale tokamaks a divertor is used to absorb the energy and trap the ash particles. As such the divertor is exposed to very high heat fluxes. This extreme heat flux limits material selection to those with a high melting point and good thermal conductivity.⁷

In addition to the heat flux, the impact of energetic particles from the plasma can cause sputtering and erosion. If sputtered particles enter back into the plasma radiative losses from electron transitions in a high atomic number (Z) material will result in cooling of the plasma. To maximise performance this loss of energy must be minimised and so either low Z material (e.g. carbon) must be used or a material with a high sputtering energy.

Further requirements for materials selection come from the neutrons produced by the fusion reaction. These high-energy (14.1 MeV) neutrons exit the plasma, as they are not constrained by the magnetic field, and interact with the structure of the reactor. When interacting with material the neutrons cause displacement damage and

Department of Materials, University of Oxford, Oxford, UK

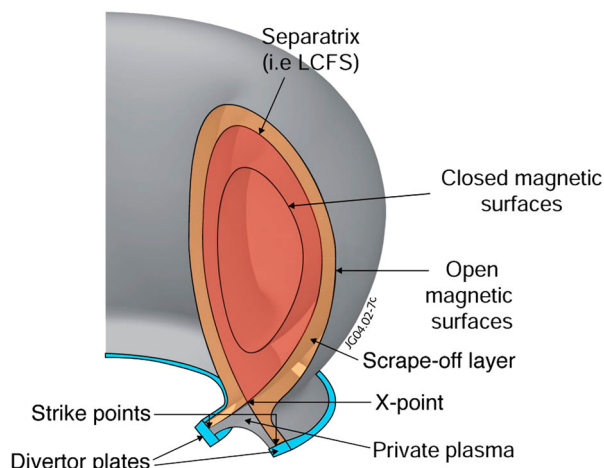
*Email: robert.abernethy@materials.ox.ac.uk

© 2016 The Author(s). Published by Informa UK Limited, trading as Taylor & Francis Group

This is an Open Access article distributed under the terms of the Creative Commons Attribution License (<http://creativecommons.org/licenses/by/4.0/>), which permits unrestricted use, distribution, and reproduction in any medium, provided the original work is properly cited.

Received 18 January 2016; accepted 20 April 2016

DOI 10.1080/02670836.2016.1185260



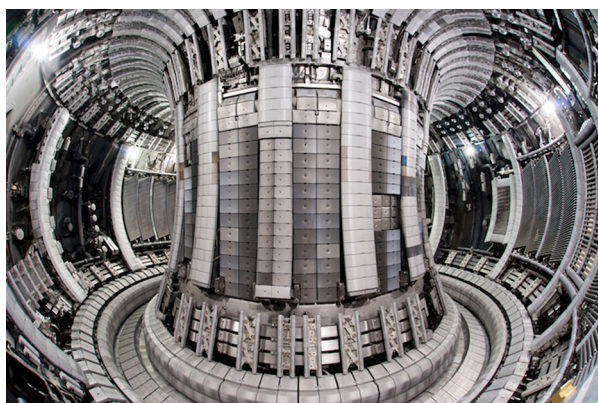
1 Diagram showing geometry of a toroidal magnetic field with a divertor. Source: Eurofusion

transmutation. As such structural materials within the reactor must be radiation resistant to avoid failure due to radiation damage and in order to minimise radioactive waste low activation materials must be used. Activation depends on the element and isotope of the original material and so certain elements are excluded from being used in a fusion reactor.⁸

Divertor materials

Carbon fibre composites were tested as a divertor material in the Joint European Torus (JET). They are made of low Z material and have high heat conductivity along the fibre axis and so seemed the optimal choice.⁹ However, chemical erosion due to reactions between the carbon tiles and hydrogen from the plasma led to more rapid erosion and concerns over the potential for tritium retention within the reactor. In order to minimise the risk from accident at a fusion reactor the tritium level must be carefully controlled and tritium retention can lead to excess.⁶ As such the carbon wall at JET was replaced with a tungsten divertor and beryllium first wall, both of which showed significantly reduced erosion.¹⁰

Tungsten was selected as a replacement for carbon due to its high energy threshold for sputtering ($E_{th} = 200$ eV for deuterium) and low erosion under high heat loads.^{6,11} It has been successfully used as the divertor material for multiple fusion experiments, such as



2 Image of JET with tungsten divertor and beryllium first wall. Source: Eurofusion

ASDEX and JET^{7,12} (see Fig. 2). As a result of this success, and the lack of suitable alternatives for fusion reactors, it has been selected as the divertor material for the next large tokamak ITER and is likely to be used as the divertor, and possibly the first wall material, for commercial-scale fusion devices.¹³

However, the challenges in advancing our ability to engineer tungsten components as well as understanding its behaviour within a fusion environment are considerable. Tungsten will be operating between 773 and 1723 K depending on location and reactor design.⁷ These high temperatures improve the ductility of tungsten but make studying tungsten under fusion-relevant conditions difficult. Two key challenges for developing tungsten have been identified as fabrication of structural divertor components and developing a complete picture of the irradiation performance of tungsten.¹⁴ This review is focussed on the latter of these two challenges, in particular on the prediction of the performance of tungsten under irradiation from fusion neutrons.

Radiation damage in tungsten

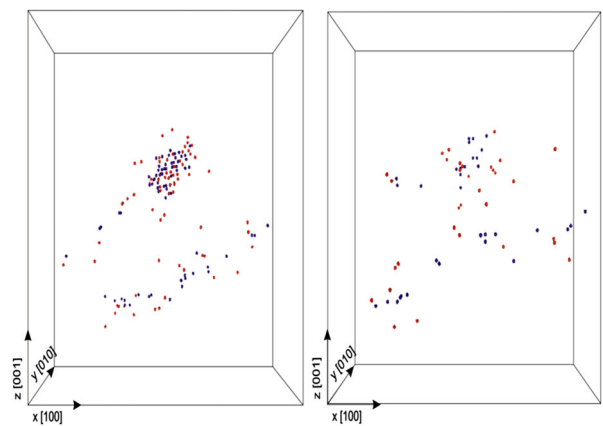
Most of the energy produced from the fusion reaction is contained within the 14.1 MeV neutron. This neutron is not constrained by the magnetic field and collides with the inner structure of the fusion reactor. Each neutron causes a damage cascade within the material, which results in an excess of vacancies and interstitial atoms. During the lifetime of a fusion reactor the damage level is expected to build up to several displacements per atom (dpa). As well as this direct damage, the neutrons also cause transmutation resulting in a build up of impurity elements within the material.¹⁵ These forms of primary damage lead to changes in microstructure, which in turn affect the thermal and mechanical properties of the material.

Cascades

The critical interaction between a neutron and a material occurs when the neutron interacts with an atom, transferring a significant portion of the energy of the neutron into producing a primary knock-on atom (pka). This atom is displaced from its lattice site and goes on to collide with other atoms, displacing them from their lattice sites, while the neutron goes on to collide elsewhere and produce multiple pkas.

Owing to the small time and length scales (events occurring on the nanometre scale as rapidly as a picosecond) modelling gives the best insight into how a material behaves during and shortly after a cascade. Stopping range in the matter model is frequently used to give an estimate of dpa.¹⁶ This model counts every atom that is displaced from its lattice site. A large excess of vacancies and interstitials are produced by a cascade, and so many will annihilate within a short time after the initial cascade (as shown in Fig. 3, taken from molecular dynamics modelling), resulting in a much smaller number of interstitials and vacancies than the dpa would suggest.¹⁷

Density functional theory (DFT) models are used to predict the structure of vacancies and interstitials that result from the cascade.¹⁸ The information from these models is somewhat limited since DFT calculations assume a temperature of 0 K, this is of particular concern for the high-energy collision cascades where the conditions are far from equilibrium. The values resulting



3 Evolution of damage cascades in Tungsten at 5 ps after collision (left) and after 30 ps (right) showing vacancy and interstitial distributions¹⁷

from DFT calculations are used in molecular dynamics and other models to understand the evolution of the microstructure shortly after the cascade occurs.

Dislocation loop and void formation

While most interstitials and vacancies will annihilate with each other shortly after the original cascade (as shown in Fig. 3), those left over can accumulate to form dislocation loops. Previously it had been thought that only loops of $b = 1/2\langle 111 \rangle$ would form¹⁹ due to the elastic isotropy of tungsten,²⁰ however recent experiments showed the existence of $b = \langle 100 \rangle$ loops as a result of irradiation at 773 K.²¹ Molecular dynamics simulations were later carried out and matched the experimental results,²² however this highlights the shortcomings of models of irradiation damage as a predictive tool.

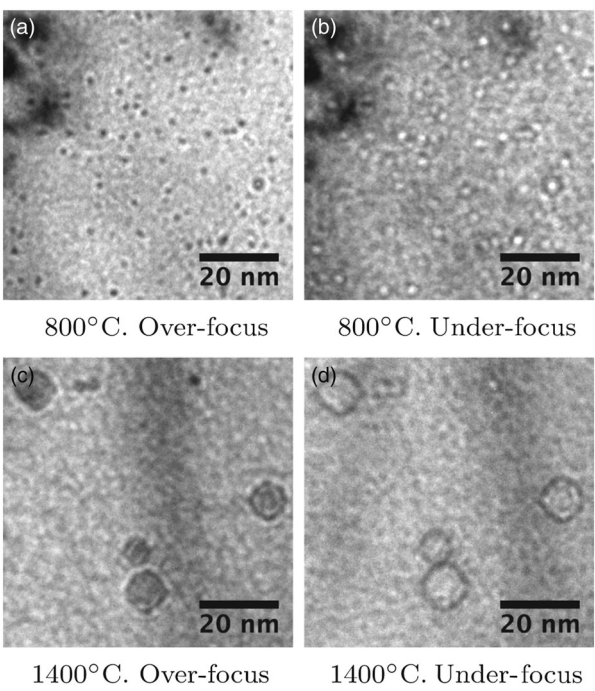
Dislocation loops in themselves act as barriers to dislocation motion and as a result contribute to radiation hardening of the material.²³ However, they are also metastable with respect to larger defects such as voids, as a result at higher temperatures, where vacancy mobility is sufficiently high, void formation is commonly observed and leads to swelling.²⁴ Body-centred cubic metals, such as tungsten, show significantly lower swelling rates than face-centred cubic metals^{25,26} and hence are preferred for applications where irradiation doses are high, but void formation is still commonly observed (see Fig. 4).²⁷

Transmutation

In addition to displacement damage neutrons are absorbed by the material and cause transmutation. In tungsten the main transmutation products are rhenium, osmium and tantalum²⁸ (see Table 1), in addition some hydrogen and helium are formed, which have a significant impact on properties.

Rhenium has potential benefits while in solution including improving the ductility²⁹ and under normal circumstances would not form the brittle χ or σ phases while concentrations are below 30 wt-% (see Fig. 5). However, the presence of osmium favours the formation of the intermetallic phases and irradiation-induced segregation has been observed.³¹

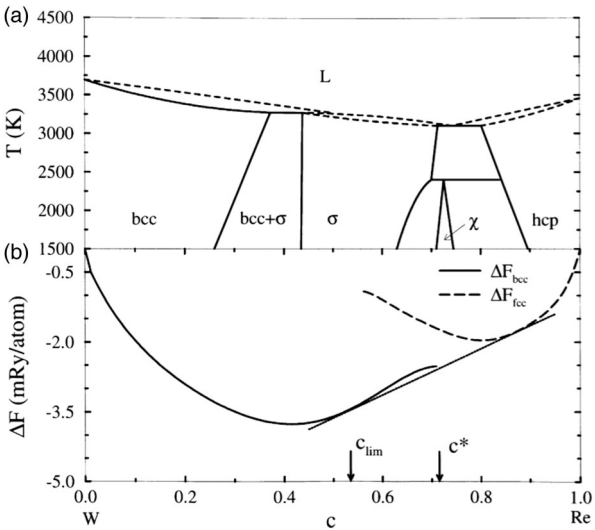
Helium formed by transmutation can act to stabilise defects produced by irradiation, this is enhanced by the



4 TEM images of voids in tungsten (taken from Ferroni et al.²⁷)

Table 1. Elemental composition of tungsten after five years in a fusion power plant²⁸

	Concentration (at.-%)
Tungsten	94.0
Rhenium	3.8
Osmium	1.4
Tantalum	0.8
Helium	34 appm
Hydrogen	76 appm



5 Phase diagram and Helmholtz free energy curves for W-Re (taken from Ekman et al.³⁰)

exposure to helium from the plasma that can diffuse into the material at high temperatures. The results include enhancing void (or bubble) formation within tungsten³² and can lead to surface blistering.

Effects of radiation damage on tungsten

The primary concern for the effect of radiation damage on tungsten are changes in thermal conductivity and radiation embrittlement. If tungsten is to be used as a structural material the operating temperature of the reactor must be above the BDTT, which increases as a result of radiation damage. The combined effect of reduced thermal conductivity and irradiation embrittlement can lead to cracking as a result of the thermal cycling that tungsten will be exposed to in a fusion reactor.¹⁴

Investigation techniques

There are many techniques used to analyse radiation damage in materials. This ranges from microscopy to large-scale mechanical testing. This review is focussed on small-scale testing techniques. Using micron-scale tests minimises the volume of material needed for analysis, this allows active samples to be examined with minimum risk. In addition ion irradiation is used as a surrogate for neutron irradiation, but only penetrates a few microns into the material. Micromechanics allow test results from ion irradiation to be compared to neutron irradiation directly.³³

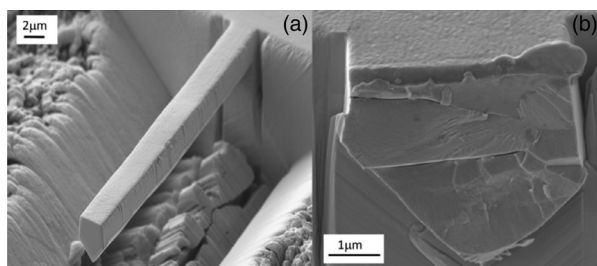
Microstructure analysis

Transmission electron microscopy (TEM) allows for direct observation of irradiation damage on the nanometre scale.³⁴ By using TEM, images of the defects can be acquired alongside diffraction patterns from the same area. This allows for the identification of the orientation of dislocation loops and using under- and over-focus voids can be identified. In addition, any precipitates can be identified along with their crystal pattern.

Micromechanics

Nanoindentation is the basis of micromechanical testing. Nanoindenters allow for force–displacement measurements on a sub-micron scale. The simplest measurement possible using this technique is a simple hardness calculation, calculated by force applied divided by contact area, which can be usefully applied to measure irradiation hardening of a material. Furthermore, elastic modulus can be calculated using the Oliver and Pharr method.³⁵

In order to enhance the data acquired from nanoindentation, it is possible to carry out micro-pillar or micro-cantilever tests.^{33,36} These forms of testing provide additional information regarding plastic deformation and fracture mechanics (see Fig. 6).



6 Fracture testing of micro-cantilever in tungsten (taken from Armstrong *et al.*³³)

Recent studies

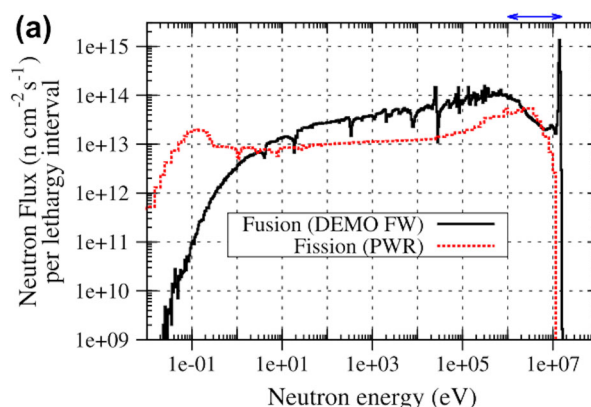
There has been a significant body of work on tungsten in recent years; this is in the build up to ITER using a tungsten divertor and during the DEMO design phase in order to predict suitable operating temperature range and device lifetime.¹⁴ Useful progress has been made, but a full understanding of the effects of irradiation on tungsten has not yet been established. The following sections summarise the state of the art.

Neutron irradiation

Neutron irradiation campaigns are limited due to the lack of availability in materials testing reactors. The cost and difficulty of irradiation are increased by the activation of the material, which results in the need to store tungsten in hot cells for several years following irradiation. Materials testing reactors typically produce a flux of fast neutrons (energies up to 2 MeV), while this does not match the mostly 14 MeV neutrons that are produced by the fusion reaction (see Fig. 7), it provides the best approximation available at present. There are plans to construct a dedicated neutron source, to mimic the materials damage caused by a fusion reactor, referred to as the International Fusion Materials Irradiation Facility (IFMIF).³⁸ This would function by firing a beam of energetic deuterons at a lithium target to produce neutrons with a broad energy peak around 14 MeV, but at present there is no planned date for completion of IFMIF.

Early neutron irradiation studies of tungsten determined the recovery stages of irradiated tungsten,³⁹ described void formation and swelling,⁴⁰ and showed irradiation-induced precipitation of the χ phase in tungsten–rhenium alloys.⁴¹ During this period of research tungsten was not being investigated as a structural material but was used as a high-temperature thermocouples for fission reactors, as a result the focus was largely on changes in electrical conductivity. Some very limited mechanical testing data were acquired during early proposals for the use of tungsten in novel reactor designs;⁴² these results showed irradiation hardening and embrittlement of tungsten.

During the early 1990s, tungsten was proposed as a potential material for the ITER divertor,⁴³ following this there was a revival in research into the properties of irradiated tungsten. Since then this renewed line of



7 Neutron spectra for a fusion power plant and current fission reactors (taken from Gilbert *et al.*³⁷)

research has continued to rise, as carbon fibre composites have been ruled out as a plasma-facing material due to tritium retention concerns,⁴⁴ and JET has performed well with the ITER-like wall, featuring a tungsten divertor. Since then neutron irradiation of tungsten has been carried out in several different locations, including JOYO and JMTR in Japan and the High Flux Isotope Reactor (HFIR) in the USA between 2005 and 2015.^{45,46} The samples from these irradiations have been analysed using TEM, electrical resistance measurements and nanoindentation. A summary of the results is presented below.

Microstructure changes

As commented above, early TEM work on neutron-irradiated tungsten–rhenium revealed the irradiation-induced segregation effect, this had previously been observed in multiple other alloys⁴⁷ and provided a significant contribution to the irradiation-induced decalibration of W-Re thermocouples. Williams *et al.*⁴¹ investigated tungsten samples irradiated in Experimental Breeder Reactor II (EBR-II), USA. Their results showed that multiple morphologies of intermetallic precipitates had formed (see Fig. 8) and that these were surprisingly χ phase rather than the lower rhenium content σ phase; several explanations for this had been proposed including that the sigma phase is disfavoured due to its slow formation and that irradiation damage can act as a stirring action favouring dissolution of the σ phase due to its high ordering energy, low defect mobility and near equiatomic composition.

Herschitz and Seidman⁴⁸ carried out further investigations into W-10 wt-% Re irradiated in EBR-II at 848, 898 and 948 K. The damage level was 8.6 dpa at a rate of 1.4×10^{-7} dpa s⁻¹. Using a field ion microscope–atom probe they showed that WRe precipitates had

formed homogeneously and that no voids formation was detected, indicating that Re suppressed void formation.

Nemoto *et al.*⁴⁹ published work in 2000 on tungsten–rhenium irradiated in the Fast Flux Test Facility (FFTF), USA, at temperatures between 646 and 1073 K and damage levels between 2 and 11 dpa. Using TEM dark field imaging they show the presence and morphology of σ and χ phase precipitates with equiaxed and lenticular morphology, respectively. This contradicted the work by Williams *et al.* which only found the χ phase to be present,⁴¹ however Williams *et al.* were only able to analyse the structure of larger precipitates formed at temperatures of 1373 K or above which may account for the difference in observations.

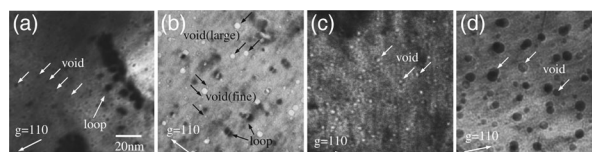
Tanno and others also at the Tohoku University produced several papers^{31,45,50–52} based upon irradiation of W–Re–Os alloys of various compositions in JOYO, Japan, at temperatures between 673 and 1023 K to damage levels of up to 1.5 dpa (the damage level increased with temperature since the length of irradiation was constant and neutron flux is the highest in the hottest regions of the fast fission reactor). Each successive paper contained more sophisticated TEM analysis; however, there were no measurement of the resultant compositions following transmutation from neutron irradiation. No precipitate formation was detected in the initially pure tungsten, but voids and dislocation loops were observed across the temperature range (see Fig. 9). Mean void size increased with temperature from 1.5 nm at 673 K, 0.17 dpa to 5 nm at 1023 K, 1.54 dpa with a void lattice possibly being detected at the highest temperature and dose (a Fourier transform of the micrograph could confirm this).

The samples containing rhenium and osmium were intended to measure the effect that transmutation would have on the behaviour of tungsten in a fusion reactor. However, the transmutation that occurred during the irradiation was not calculated or measured, and so the final composition is not exactly known. It is stated that the transmutation of tungsten in fast reactors is negligible by Tanno *et al.*,^{31,51} based upon a repeatedly misprinted citation to Greenwood and Garner.⁵³ However, a later paper by the same authors shows an extremely strong dependence of transmutation rate on the neutron spectrum, which fluctuates with the location of the sample within the fast reactor,⁵⁴ as such assuming negligible transmutation may not be valid since the spectrum from JOYO is simply assumed to be similar to that of FFTF. In addition Williams *et al.* observed the transmutation of tungsten in a fast reactor.⁴¹

The authors also fail to detail the dose rate, length of irradiation, location in the reactor and during which cycles of the reactor the irradiation took place; thus, the



8 TEM micrograph showing both acicular and circular precipitates formed by neutron irradiation of W-11Re at 1173 K⁴¹



9 TEM micrographs showing voids in tungsten irradiated at a 0.17 dpa at 673 K, b 0.96 dpa at 701 K, c 0.40 dpa at 1013 K and d 1.54 dpa at 1023 K⁵¹

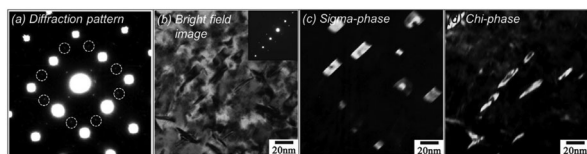
accuracy of the data about the irradiation that is provided cannot be ascertained. This contrasts strongly with the approach by Nemoto *et al.*⁴⁹ who provided cycle number, such that the length of irradiation and hence dose rate can theoretically be calculated, as well as temperature control accuracy. All the data from FFTF are far better documented, with reports on irradiation conditions available online for each Materials Open Test Assembly.

It was shown that initial rhenium content of 5 wt-% or Os above 3 wt-% and above suppressed void formation (also some were observed in W-Re alloys at higher levels) and resulted in precipitate formation. The precipitates were again characterised into two types, equiaxed and platelet (assumed to be σ and χ phase, respectively, based on the work of Nemoto *et al.*⁴⁹).

The work by Tanno *et al.* was the most extensive part of a series of work carried out in Japan analysing tungsten and tungsten–rhenium irradiated in various reactors. He *et al.* carried out analysis of tungsten samples irradiated in the Japan Materials Testing Reactor (JMTR),⁵⁵ at 873 and 1073 K to a damage level of 0.15 dpa. They showed voids and loops formed by irradiation showing that void size increased with temperature and void density decreased with rhenium content. They detected no irradiation-induced segregation. The JMTR (a mixed spectrum reactor) has a significantly different neutron spectrum to FFTF and JOYO (which are both fast reactors), as such the thermal component of the neutron spectrum will be much higher causing significantly higher transmutation per dpa. As a result of this direct comparison of results from these two different neutron sources should be approached with caution. He *et al.* gave no details of the spectrum and no estimate of error in temperature measurements during the irradiation.

Fukuda *et al.* carried out analysis of samples irradiated in the High Flux Isotope Reactor, USA (HFIR).⁴⁶ Their irradiation conditions were 0.9 dpa at 773 K and 0.98 dpa at 1073 K. Using FISPACT they calculated the transmutation which showed that initially pure tungsten had a final composition of W-9%Re-5%Os. However, they did not produce experimental results to verify these computations, but this does highlight the issue in earlier papers not calculating transmutation levels due to irradiation.

Their analysis of initially pure tungsten showed void formation in at 1073 K and dislocation loops at 773 K, along with precipitate formation in both cases. Precipitates were observed in all samples and precipitate size increased with temperature and number density increased with initial rhenium content. They repeated the analysis of Nemoto *et al.*,⁴⁹ showing that both σ and χ phase precipitates were present with equiaxed and platelet morphology, respectively (see Fig. 10).



10 TEM micrographs showing pure tungsten after irradiation to 0.98 dpa at 1073 K: a diffraction pattern from (001), b bright-field image, and c and d dark-field images of precipitates⁴⁶

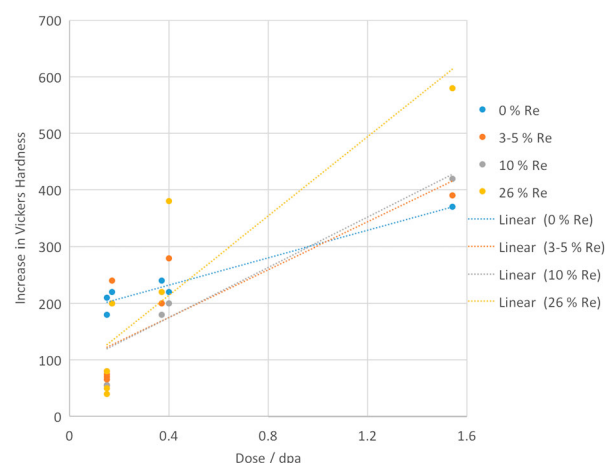
Effect on properties

In addition to TEM analysis most of the recent work from Japan cited above included hardness measurements and some involved electrical resistivity measurements. He *et al.* measured the change in Vickers hardness (ΔHV) across several irradiation conditions. They showed at 0.15 dpa (where no irradiation-induced segregation was observed) that pure tungsten ($\Delta HV \approx 175$) hardened significantly more than W- x Re ($x = 3 - 26\%$) ($\Delta HV \approx 50$) at all temperatures at 873 and 1073 K. In contrast Tanno *et al.*⁴⁵ presented results showing consistent hardening for pure tungsten and W- x Re of $\Delta HV \approx 200$ at 0.17 dpa at 673 and 773 K.

The key differences between the studies are the temperature ranges and the reactor type. At higher temperatures annealing of radiation damage is more probable and so this may account for the lower increase in hardness on average observed by He *et al.*, however the result for pure tungsten then becomes an anomaly. He *et al.* used a mixed neutron spectrum for irradiation and so more transmutation would be expected than for the fast neutron spectrum used by Tanno *et al.*, as such the anomalously high hardening of the pure tungsten detected by He *et al.* may be due to transmutation of W to Re and Os, which was not accounted for.

Another possible explanation for the disparity is void formation. At the higher temperature used by He *et al.* void formation would be more likely to occur. Neither author explicitly observed voids at dose levels below 1 dpa, but Hasegawa later identified them at 673 K, 0.17 dpa and 913 K, 0.4 dpa.⁵⁶ Voids are thought to be the main contributor to irradiation hardening in pure tungsten,⁴⁵ but are suppressed by rhenium content; in rhenium containing tungsten alloys precipitation formation is thought to be the primary contributor to irradiation hardening. This change in the hardening mechanism may explain the change in temperature dependence of different alloys.

At 1023 K, 1.5 dpa irradiation hardening was shown to increase with increasing rhenium content.⁴⁵ This indicates that above 1 dpa irradiation-induced segregation exceeds



11 Increase in hardness of W- x Re with increase neutron dose across a range of temperatures, increasing rhenium content increases the rate of hardening due to precipitate formation. Reproduced with data from Tanno *et al.*⁴⁵ and He *et al.*⁵⁵

the contribution to hardening from void formation, which is thought to saturate upon the formation of the void lattice;⁵⁷ data for irradiation of W-*x* % Re are summarised in Fig. 11. Tanno also demonstrated that osmium content dramatically increased hardening, especially for low rhenium content, to $\Delta 600$] > for W-3% Os even at < 1 dpa. This may be because osmium encourages the formation of W-Re-Os precipitates.

Summary of neutron-irradiated tungsten

The phenomenon of irradiation-induced segregation has been clearly observed in tungsten under neutron irradiation, especially when Re and/or Os are present before the irradiation. It appears to occur across a broad range in temperatures and result in σ and χ phase precipitates formation. The exact conditions are somewhat unclear due to inconsistencies in calculating or measuring transmutation due to neutron irradiation. Void formation is observed in pure tungsten but is suppressed by Re and Os content.

Irradiation hardening has been measured in a broad range of W-Re-Os alloys under various conditions. It is associated with void formation in pure tungsten and precipitate formation in Re or Os containing samples. Hardening due to void formation appears to saturate around 1 dpa, but saturation in hardening due to precipitates formation has not yet been observed.

There are some criticisms of the current data available from neutron irradiation of tungsten. Most irradiation has occurred below 1000 K so data for fusion divertor-relevant temperatures are limited. In addition to this the only mechanical testing has been microindentation carried out at room temperature, so the effect of voids or precipitates on high-temperature mechanical properties is not yet known. Only hardness increases have been measured so understanding of the change in fracture properties of tungsten, which are critical for use as a structural material, is yet to be developed. In addition, characterisation of the dislocation loops caused by neutron irradiation has not been carried out.

Ion irradiation

Ion irradiation has been used for several decades to simulate the effect of neutron damage on metals.⁵⁸ It has been used for multiple reasons: to separate effects due to direct displacement damage from those caused by transmutation and gas evolution, to accelerate materials testing to extremely high dpa levels,⁵⁹ and simply to avoid the additional cost and difficulty of neutron irradiation.⁶⁰ In order to best simulate the direct damage caused by fast neutrons, high-energy ions are used such that the main stopping force is due to direct collisions as opposed to electronic interactions, which dominate at low energies (< 1 MeV).

The main disadvantage to ion irradiation is the shallow damage profile produced since ions only penetrate a few microns into a material (precise depth depends on energy used and *z* number of the material). TEM investigations only probe a few hundred nm depth of sample so this is not a concern, however for mechanical testing novel methods for probing the irradiated layer have only been developed in recent years.³³

Microstructure changes

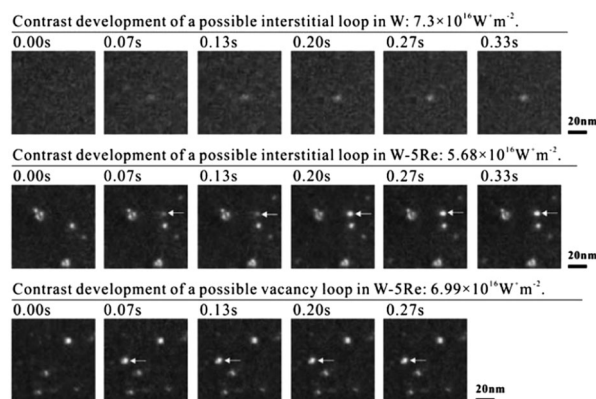
Field ion and electron microscopy of radiation damage in tungsten was carried out during the late 1960s and was summarised by Buswell.⁶¹ All of this work was carried out using low energy irradiation (< 1 MeV) but showed the presence and proportion of small vacancy clusters (< 10 vacancies per cluster, 80% of damage), irregularly shaped voids (up to 300 vacancies per cluster), and dislocation loops ($b = 1/2\langle 111 \rangle$ or $b = 1/3\langle 112 \rangle$, less than 10% of damage).

Eyre and Bullough⁶² provided a mechanism for the formation of $1/2\langle 111 \rangle$ and $\langle 100 \rangle$ dislocation loops in BCC metals. Jäger and Wilkens⁶³ using TEM of tungsten irradiated with 60 keV Au ions, showed that the mechanism proposed by Eyre and Bullough could explain the formation of the observed $1/2\langle 111 \rangle$ vacancy loops. This work relied on a previous paper published by Häussermann *et al.*⁶⁴ analysing the butterfly contrast observed in TEM and measuring loop orientation based upon this contrast and the diffraction conditions.

The most significant work on TEM of ion-irradiated tungsten since this has been conducted by Yi *et al.*²¹ In this work *in situ* irradiation at 773 K was used to understand the evolution of the microstructure during ongoing irradiation. This allowed observation of the formation of dislocation loops. It was found that interstitial loops form slowly as a result of migration of interstitials, whereas vacancy loops form almost instantly as a result of cascade collapse (see Fig. 12).

Information on loops formation such as this is crucial for validating predictions from molecular dynamics simulations, which can then, in turn, provide much greater insight into how radiation damage occurs and critically how it will extend to other experimental conditions and how its effect might be minimised. $\langle 100 \rangle$ loops were also observed, having not been observed by Häussermann *et al.*, this may be due to the higher temperatures since faulted $\langle 110 \rangle$ loops were not observed by Yi *et al.* but were observed by Häussermann *et al.* This is an important observation for understanding the behaviour of tungsten at fusion-relevant temperatures.

Yi *et al.* also provide important information on the effect of rhenium. First, it was shown that W-5% Re may increase the defect yield by reducing the stacking fault energy and thus stabilising the initial faulted loops



12 TEM micrographs showing steady formation and growth of interstitial loops over 0.3 s and sudden appearance of vacancy loops²¹

that form on $\langle 110 \rangle$. However, it was also shown that rhenium retards the motion of $b = 1/2\langle 111 \rangle$, which may explain how rhenium suppresses void formation.

Ferroni *et al.*²⁷ used TEM to characterise the different stages of recovery in irradiated tungsten. Previous studies had identified different recovery regimes based upon electrical resistivity measurements³⁹ but the underlying change in microstructure had not been directly observed. Five stages of recovery were identified: (1) < 573 K No dislocation loop motion, (2) 573–973 K one-dimensional hopping of small loops, (3) 973–1073 K Loops reorganise into chains or clusters, (4) 1073–1273 K coalescence of loops into finger loops, and (5) sweeping out of dislocation loops by line dislocations and void formation. It was noted by Ferroni that during stage 5 dislocation loops break into line dislocations only upon encountering the surface, as such the behaviour of bulk behaviour may be significantly different to the 100 nm thick TEM foil.

Xu *et al.*⁶⁵ carried out an atom probe study into ion-irradiated W–2% Re and W–1% Re–1% Os. Irradiations were carried out at 573 and 773 K to 33 dpa. Significant clustering was observed in all samples; however, in Os containing samples the segregation of Re was suppressed, possibly due to Os preferentially binding to vacancies. Armstrong *et al.*⁶⁶ irradiated W–5% Re at 573 K to a range of doses from 0.07 to 33 dpa. Significant clustering was only observed at the higher doses examined (13 and 33 dpa) and not at 1.2 dpa.

Effect on properties

Owing to the difficulties in probing the small volume of irradiated material produced by ion irradiation, it has only recently been possible to investigate mechanical properties within ion-irradiated material. This has been facilitated by advances in nanoindentation, and understanding the deformation induced by indentation,⁶⁷ and by the development of novel techniques using focussed ion beam to mill out mechanical testing samples, such as cantilevers and pillars, on a micron scale.³³

The primary work on tungsten has been carried out by Armstrong^{66,68} investigating W, W–5% Re and W–5% Ta irradiated between 0.07 and 33 dpa at 573 K. The data from his work are summarised in Fig. 13. At low doses (up to 1 dpa) hardening is similar, however hardening of pure tungsten saturates around 1 dpa whereas W–5% Re and W–5% Ta continue to increase in hardness up to 33 dpa. This was shown to be associated with clustering of

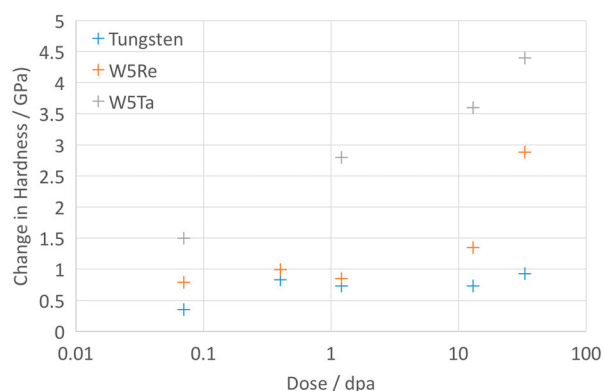
the rhenium in W–5% Re and is likely to be caused by a similar mechanism in W–5% Ta.

Gibson *et al.*⁶⁹ tested the behaviour of micro-cantilevers in ion-irradiated tungsten and compared the results with nanoindentation of the same samples. The implantation was carried out at 1073 K to approximately 2 dpa. Owing to the large error in acquired results it is difficult to draw any firm conclusions, however, a larger increase in hardness from nanoindentation was observed compared to the increase in yield stress from micro-cantilever bend tests. This may be an indication that dislocation sources have not been effected by irradiation but that dislocation motion is impeded by irradiation damage, since nanoindentation produces large local stresses such that dislocations can nucleate homogeneously whereas cantilever testing will only activate already present dislocation sources.

While micromechanics of ion-irradiated material can provide critical information about behaviour of tungsten under irradiation much more rapidly and at lower expense than neutron irradiation, care must be taken since there are numerous factors that may complicate the results. One prominent issue is the indentation size effect as described by Nix and Gao.⁷⁰ This is a result of hardness appearing to increase with decreasing size, possibly because of the relatively low number of dislocation sources within the stressed volume. This becomes further complicated when combined with a variable level of irradiation damage caused by ion irradiation and steps that should be taken towards mitigating any possible errors are provided by Hosemann *et al.*⁷¹

Summary of ion irradiation

Ion irradiation has successfully been used in combination with TEM studies to provide a significant insight into the formation of radiation defects in tungsten. Loop formation and annealing effects have been well characterised, and crucial information on the effect of transmutation on damage formation has been gained. These results can be used to improve modelling of the evolution of radiation damage and improve the understanding of the fundamental factors in irradiation damage. While ion irradiation provides a much easier method for analysing radiation damage in tungsten, there are some points of concern. The differences observed between results in ion and neutron irradiation experiments are highlighted in section ‘Embrittlement of Tungsten’. One key issue is the effect of the large difference in dose rate between ion and neutron irradiation, which is not well understood. In addition to the indentation size effect for mechanical testing highlighted above, the effect of free surfaces, especially during *in situ* irradiation, should be carefully considered and accounted for. When it comes to understanding mechanical properties using ion irradiation, the difficulty in analysing deformation in a small near-surface volume remains significant. However, the developments in micromechanics certainly offer significant potential for determining changes in properties such as yield stress and elastic modulus. These techniques currently need further refinement to reduce the errors involved and a greater understanding of the indentation size effect in irradiated material is required.



13 Hardening of tungsten and tungsten alloys under self-ion irradiation^{66,68}

Helium in tungsten

The effect of hydrogen and helium on tungsten in a fusion environment is a considerable concern. Low levels of helium and hydrogen (34 and 76 appm after five full power years, respectively) are expected to be evolved from the interaction between high-energy neutrons and tungsten in a fusion reactor.²⁸ A far more significant source is surface exposure to the hydrogen and helium plasma, which results in a high-flux low-energy helium ion implantation.

This surface exposure to helium containing plasmas has been observed to result in the formation of tungsten fuzz.⁷² In addition, the high temperatures of the fusion environment will result in helium diffusing deep into the material, where it interacts strongly with radiation damage.⁷³

Tungsten fuzz formation

Exposure to a helium plasma results in the formation of tungsten fuzz (see Fig. 14). This effect was first discovered in 2006⁷⁴ and later observed on several plasma devices and different grades of tungsten.⁷² It forms at temperatures over 1000 K and helium fluxes in excess of 10^{24} m^{-2} .⁷⁵ *In situ* TEM observations and molecular dynamics models have shown that helium accumulates in clusters that grow into bubbles. Bubbles close to the surface then rupture producing the fuzz structure.^{76,77}

There are concerns of the effect of tungsten fuzz on divertor performance for future fusion devices. One primary concern was that the formation of tungsten fuzz would increase sputtering rates, this would result in tungsten impurities with the plasma, which cool the plasma and would prevent fusion being achieved. However, sputtering experiments showed that tungsten fuzz formation significantly reduced the sputtering rate.⁷⁸ Concerns yet to be addressed include thermal performance of tungsten fuzz and the survivability of tungsten fuzz during transient events such as disruptions.

Effect of helium on irradiation damage

DFT models show that helium interacts strongly with vacancies within tungsten.⁷³ This has been confirmed experimentally through measurements of lattice swelling.⁷⁹ This interaction may radically alter the behaviour of irradiation damage in tungsten and is likely to favour the formation of bubbles/voids. Studies concerning both

irradiation damage and helium implantation are relatively few in number.

Armstrong *et al.*⁸⁰ carried out tungsten self-ion irradiation to 13 dpa followed by helium implantation to 3000 appm at 573 K. Hardness measurements were carried out by nanoindentation, the results are shown in Fig. 15. The hardening effect from displacement damage of self-ions can be clearly seen. He implantation causes a much larger increase in hardness, due to helium embrittlement, but seems to be mitigated by the presence of irradiation damage. This suggests that helium is being trapped by radiation defects and no longer contributes to hardening. Gibson *et al.*⁸¹ carried out high-temperature indentation of helium-implanted tungsten and showed that the hardening effect was significantly decreased at 673 K and above.

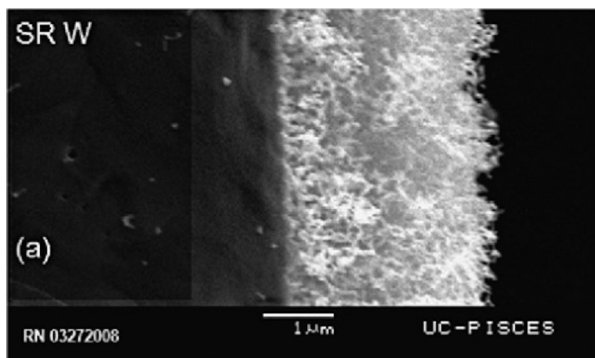
Future work

Overall there are still many unanswered questions as to the performance of tungsten within a fusion environment. Some of the key gaps in the existing literature for experimental work on irradiated tungsten have been identified below.

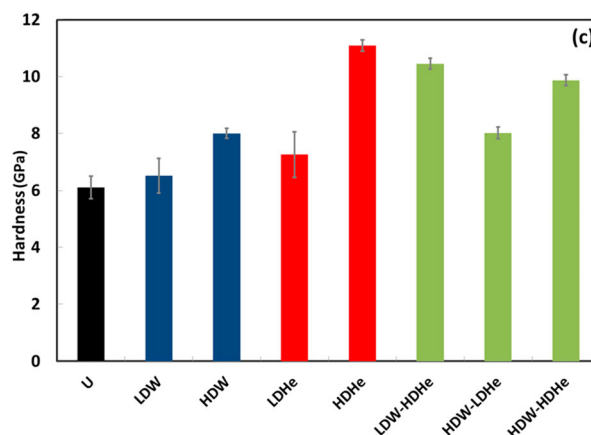
Embrittlement of tungsten

The combined effect of helium, neutron irradiation and high temperatures has not yet been determined and further study is still required. One important parameter that has not yet been investigated for irradiated tungsten is the brittle to ductile transition temperature (BDTT). Irradiation has been shown to increase the BDTT in ferritic-martensitic steels⁸² and so is expected to have a similar impact on tungsten.

The BDTT in tungsten has been shown to be associated with the kink pair mechanism for motion of screw dislocations⁸³ and so is dependent on dislocation motion rather than nucleations.⁸⁴ Although it is not immediately apparent as to how this mechanism would change as a result of irradiation damage, the work by Gibson *et al.*⁶⁹ suggested that irradiation damage was impeding dislocation motion, rather than reducing source activity, as so an increase in BDTT would be expected.



14 Tungsten fuzz formed by exposure to He containing plasma on PISCES B⁷²



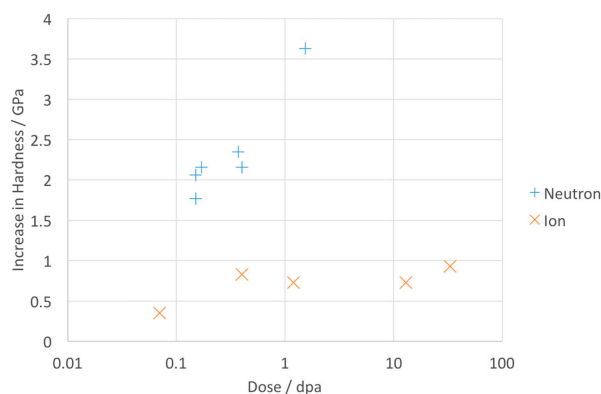
15 Hardness measurements from tungsten irradiated with self-ions to 0.02 dpa (LDW) or 0.25 dpa (HDW) and He to 300 appm (LDHe) or 3000 appm (HDHe)⁸⁰

This increase in BDTT is particularly critical for the use of tungsten within a fusion reactor. Although tungsten will be operating at high temperatures as a plasma-facing material, the outer side must be sufficiently cool to allow for a structural heat sink material, likely copper based, to be joined directly to the tungsten. The minimum operating temperature of tungsten will be dependent upon its BDTT following irradiation, and so a thorough study repeating the work of Giannattasio *et al.*⁸³ to investigate any change in dislocation behaviour following irradiation would be prudent.

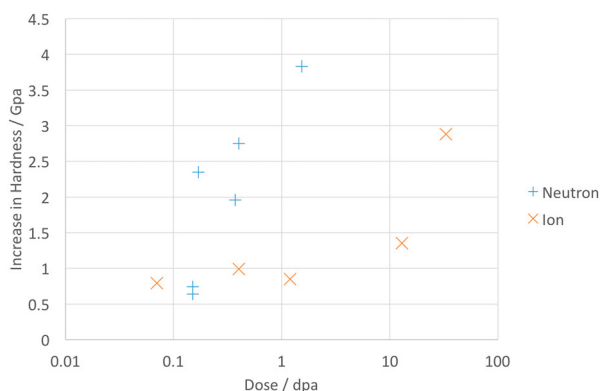
Comparing ions and neutrons

Ion irradiation is used primarily as a surrogate for neutron irradiation, however, results from neutron and ion irradiation in tungsten are not well correlated. For example, the results of hardness testing from ion and neutron irradiation are presented in Figs. 16 (Pure tungsten) and 17 (W–5% Re). It is clear from these graphs that a higher level of irradiation hardening is observed for neutron irradiation than ion irradiation. This is particularly confusing since the ion irradiation took place at a lower temperature.

In order to reconcile these data there are several possible explanations. First, transmutation due to neutron exposure has not been accounted for, this would explain why the difference between neutron and ion irradiation appears greater in pure tungsten than W – 5% Re.



16 Hardness measurements comparing ion and neutron irradiation for pure tungsten^{45,55,66}



17 Hardness measurements comparing ion and neutron irradiation for W–5% Re^{45,55,66}

Table 2. Hardness measurements of W and W–5% Re before irradiation^{66,86}

	Author	Fabrication	Hardness/ GPa
Tungsten	Armstrong	Plansee	7.62
Tungsten	He/Tanno	Arc Melted and Annealed	3.72
W–5% Re	Armstrong	Arc Melted and Annealed	6.45
W–5% Re	He/Tanno	Arc Melted and Annealed	3.23

Second, although at a higher dose rate there is less time of radiation damage to be annealed and so greater increases in hardness would be expected, investigations in Fe–Cr systems have shown that greater segregation occurs at lower dose rates,⁸⁵ resulting in larger increases in hardness. This would explain the lower increase in hardness for the ion-irradiated W–5% Re and matches the microstructural observations where clustering was only observed for the ion irradiated W–5% Re at > 10 dpa whereas precipitates were observed in W–5% Re at around 1 dpa.⁵¹

Finally, the difference in measurement of hardness, microindentation compared to nanoindentation, resulted in vastly different values for initial hardness and so will lead to some difference in the measurement of change in hardness (see Table 2). A careful investigation of ion- and neutron-irradiated material using the same technique would go some way to clarifying this difference and would play a critical role in validating the use of ion irradiation as a proxy for neutron irradiation across a range of materials.

Dislocation loops in neutron-irradiated tungsten

It is also striking that TEM work identifying the nature of dislocation loops in ion-irradiated tungsten²¹ is used to parameterise and validate models,²² which in turn provide an insight into the nature of displacement cascades, but has not been compared to defects in samples that have undergone neutron irradiation. Given the strong dependence of pka energy on neutron interaction type,⁸⁷ the difference in cascade evolution between collisions strongly interacting ions and more weakly interacting neutrons may produce significant differences in resultant microstructure.

Reproducing the work of Yi *et al.* on neutron-irradiated material is likely to clarify the effect of neutron irradiation on tungsten, assist with producing models to predict the effects of irradiation, and potentially help explain the differences observed between ion and neutron irradiation.

Acknowledgments

I would like to thank my supervisors Dr David Armstrong, Dr Chris Hardie and Professor Steve Roberts for their valuable input and support during this work, and to Mark Gilbert for fruitful conversations regarding neutron irradiations.

Disclosure statement

No potential conflict of interest was reported by the author.

Funding

This work was supported by EPSRC Fusion CDT grant EP/L01663X/1, alongside Culham Centre for Fusion Energy iCase award.

ORCID

R. G. Abernethy  <http://orcid.org/0000-0003-4611-9907>

References

1. IEA, 'World Energy Outlook 2015 Factsheet – Global energy trends to 2040', 2015.
2. S. Chu and A. Majumdar: 'Opportunities and challenges for a sustainable energy future', *Nature*, **Aug. 2012**, **488**, 294–303.
3. M. S. Dresselhaus and I. L. Thomas: 'Alternative energy technologies', *Nature*, **Nov. 2001**, **414**, 332–337.
4. D. J. Ward, I. Cook, Y. Lechon, and R. Saez: 'The economic viability of fusion power', *Fusion Eng. Design*, **2005**, **75–79**, 1221–1227.
5. E. E. Bloom: 'The challenge of developing structural materials for fusion power systems', *J. Nucl. Mater.*, **Oct. 1998**, **258–263**, 7–17.
6. H. Bolt, V. Barabash, G. Federici, J. Linke, A. Loarte, J. Roth, and K. Sato: 'Plasma facing and high heat flux materials – needs for ITER and beyond', *J. Nucl. Mater.*, **Dec. 2002**, **307–311**, 43–52.
7. H. Bolt, V. Barabash, W. Krauss, J. Linke, R. Neu, S. Suzuki, and N. Yoshida: 'Materials for the plasma-facing components of fusion reactors', *J. Nucl. Mater.*, **Aug. 2004**, **329–333**, 66–73.
8. S. J. Zinkle and J. T. Busby: 'Structural materials for fission & fusion energy', *Mater. Today*, **Nov. 2009**, **12**, 12–19.
9. J. Schlosser, A. Cardella, P. Chappuis, J. Coston, P. Deschamps, and M. Lipa: 'Development of high thermal flux components for continuous operation in Tokamaks', 14th IEEE / NPSS Symposium: Fusion Engineering, Proceedings, Vols. 1 and 2, 1992, 350–356.
10. S. Krat, Y. Gasparyan, A. Pisarev, I. Bykov, M. Mayer, G. de Saint Aubin, M. Balden, C. P. Lungu, and A. Widdowson: 'Erosion at the inner wall of JET during the discharge campaign 2011–2012 in comparison with previous campaigns', *J. Nucl. Mater.*, **Jan. 2015**, **456**, 106–110.
11. J. Davis, V. Barabash, A. Makhankov, L. Plöchl, and K. Slattery: 'Assessment of tungsten for use in the ITER plasma facing components', *J. Nucl. Mater.*, **Oct. 1998**, **258–263**, 308–312.
12. F. Romanelli: 'Overview of the JET results with the ITER-like wall', *Nucl. Fusion*, **Oct. 2013**, **53**, 104002.
13. R. Neu, R. Dux, A. Kallenbach, T. Pütterich, M. Balden, J. Fuchs, A. Herrmann, C. Maggi, M. O'Mullane, R. Pugno, I. Radivojevic, V. Rohde, A. Sips, W. Suttrop, A. Whiteford, and T. A. U. Team: 'Tungsten: an option for divertor and main chamber plasma facing components in future fusion devices', *Nucl. Fusion*, **Mar. 2005**, **45**, 209–218.
14. M. Rieth, S. L. Dudarev, S. M. Gonzalez de Vicente, J. Aktaa, T. Ahlgren, S. Antusch, D. E. J. Armstrong, M. Balden, N. Baluc, M.-F. Barthe, W. W. Basuki, M. Battabyal, C. S. Becquart, D. Blagoeva, H. Boldyryeva, J. Brinkmann, M. Celino, L. Ciupinski, J. B. Correia, A. De Backer, C. Domain, E. Gaganidze, C. Garcia-Rosales, J. Gibson, M. R. Gilbert, S. Giusepponi, B. Gludovatz, H. Greuner, K. Heinola, T. Höschen, A. Hoffmann, N. Holstein, F. Koch, W. Krauss, H. Li, S. Lindig, J. Linke, C. Linsmeier, P. López-Ruiz, H. Maier, J. Matejicek, T. P. Mishra, M. Muhammed, A. Muñoz, M. Muzyk, K. Nordlund, D. Nguyen-Manh, J. Opschoor, N. Ordás, T. Palacios, G. Pintsuk, R. Pippan, J. Reiser, J. Riesch, S. G. Roberts, L. Romaner, M. Rosinski, M. Sanchez, W. Schulmeyer, H. Traxler, A. Ureña, J. G. van der Laan, L. Velea, S. Wahlberg, M. Walter, T. Weber, T. Weitkamp, S. Wurster, M. A. Yar, J. H. You, and A. Zivelonghi: 'Recent progress in research on tungsten materials for nuclear fusion applications in Europe', *J. Nucl. Mater.*, **Jan. 2013**, **432**, 482–500.
15. V. Barabash, G. Federici, J. Linke, and C. H. Wu: 'Material/plasma surface interaction issues following neutron damage', *Journal of Nuclear Materials*, **March. 2003**, **313–316**, 42–51.
16. R. E. Stoller, M. B. Toloczko, G. S. Was, A. G. Certain, S. Dwaraknath, and F. A. Garner: 'On the use of SRIM for computing radiation damage exposure', *Nuclear Instruments and Methods in Physics Research Section B: Beam Interactions with Materials and Atoms*, **Sep. 2013**, **310**, 75–80.
17. T. Troev, N. Nankov, and T. Yoshiie: 'Simulation of displacement cascades in tungsten irradiated by fusion neutrons', *Nuclear Instruments and Methods in Physics Research Section B: Beam Interactions with Materials and Atoms*, **Mar. 2011**, **269**, 566–571.
18. P. M. Derlet, D. Nguyen-Manh, and S. L. Dudarev: 'Multiscale modeling of crowdion and vacancy defects in body-centered-cubic transition metals', *Phys. Rev. B*, **Aug. 2007**, **76**, 054107.
19. M. R. Gilbert, S. L. Dudarev, P. M. Derlet, and D. G. Pettifor: 'Structure and metastability of mesoscopic vacancy and interstitial loop defects in iron and tungsten', *J. Phys.: Condens. Matter*, **Aug. 2008**, **20**, 345214.
20. S. L. Dudarev, R. Bullough, and P. M. Derlet: 'Effect of the alpha-gamma phase transition on the stability of dislocation loops in bcc iron', *Phys. Rev. Lett.*, **Apr. 2008**, **100**, 135503.
21. X. Yi, M. L. Jenkins, M. Briceno, S. G. Roberts, Z. Zhou, and M. A. Kirk: 'In situ study of self-ion irradiation damage in W and W-5Re at 500°C', *Philos. Mag.*, **May 2013**, **93**, 1715–1738.
22. A. E. Sand, S. L. Dudarev, and K. Nordlund: 'High-energy collision cascades in tungsten: dislocation loops structure and clustering scaling laws', *EPL (Europhys. Lett.)*, **2013**, **103**, 46003.
23. P. Kroupa: 'The interaction between prismatic dislocation loops and straight dislocations. Part I', *Philos. Mag.*, **May 1962**, **7**, 783–801.
24. A. D. Brailsford and R. Bullough: 'The rate theory of swelling due to void growth in irradiated metals', *J. Nucl. Mater.*, **Aug. 1972**, **44**, 121–135.
25. B. Singh and J. Evans: 'Significant differences in defect accumulation behaviour between fcc and bcc crystals under cascade damage conditions', *J. Nucl. Mater.*, **Nov. 1995**, **226**, 277–285.
26. T. Lechtenberg: 'Irradiation effects in ferritic steels', *J. Nucl. Mater.*, **Aug. 1985**, **133–134**, 149–155.
27. F. Ferroni, X. Yi, K. Arakawa, S. P. Fitzgerald, P. D. Edmondson, and S. G. Roberts: 'High temperature annealing of ion irradiated tungsten', *Acta Mater.*, **May 2015**, **90**, 380–393.
28. M. R. Gilbert and J.-C. Sublet: 'Neutron-induced transmutation effects in W and W-alloys in a fusion environment', *Nucl. Fusion*, **Apr. 2011**, **51**, 043005.
29. T. Leonhardt: 'Properties of tungsten–rhenium and tungsten–rhenium with hafnium carbide', *JOM*, **Jul. 2009**, **61**, 68–71.
30. M. Ekman, K. Persson, and G. Grimvall: 'Phase diagram and lattice instability in tungsten–rhenium alloys', *J. Nucl. Mater.*, **Apr. 2000**, **278**, 273–276.
31. T. Tanno, A. Hasegawa, M. Fujiwara, J.-C. He, S. Nogami, M. Satou, T. Shishido, and K. Abe: 'Precipitation of solid transmutation elements in irradiated tungsten alloys', *Mater. Trans.*, **2008**, **49**, (10), 2259–2264.
32. N. Yoshida: 'Review of recent works in development and evaluation of high-Z plasma facing materials', *J. Nucl. Mater.*, **Mar. 1999**, **266–269**, 197–206.
33. D. Armstrong, C. Hardie, J. Gibson, A. Bushby, P. Edmondson, and S. Roberts: 'Small-scale characterisation of irradiated nuclear materials: part II nanoindentation and micro-cantilever testing of ion irradiated nuclear materials', *J. Nucl. Mater.*, **Jul. 2015**, **462**, 374–381.
34. M. Jenkins: 'Characterisation of radiation-damage microstructures by TEM', *J. Nucl. Mater.*, **Oct. 1994**, **216**, 124–156.
35. W. C. Oliver and G. M. Pharr: 'Measurement of hardness and elastic modulus by instrumented indentation: advances in understanding and refinements to methodology', *J. Mater. Res.*, **Jan. 2004**, **19**, 3–20.
36. E. Grieveson, D. Armstrong, S. Xu, and S. Roberts: 'Compression of self-ion implanted iron micropillars', *J. Nucl. Mater.*, **Nov. 2012**, **430**, 119–124.
37. M. R. Gilbert, S. L. Dudarev, D. Nguyen-Manh, S. Zheng, L. W. Packer, and J. C. Sublet: 'Neutron-induced dpa, transmutations, gas production, and helium embrittlement of fusion materials', *J. Nucl. Mater.*, **2013**, **442**, (1–3 SUPPL. 1), S755–S760.
38. K. Ehrlich and A. Möslang: 'IFMIF – An International Fusion Materials Irradiation Facility', *Nucl. Instrum. Methods Phys. Res. Sect. B: Beam Interact. Mater. Atoms*, **Apr. 1998**, **139**, 72–81.
39. L. K. Keys and J. Moteff: 'Neutron irradiation and defect recovery of tungsten', *J. Nucl. Mater.*, **Mar. 1970**, **34**, 260–280.
40. J. Matolich, H. Nahm, and J. Moteff: 'Swelling in neutron irradiated tungsten and tungsten-25 percent rhenium', *Scr. Metall.*, **Jul. 1974**, **8**, 837–841.

41. R. K. Williams, F. W. Wiffen, J. Bentley, and J. O. Stiegler: 'Irradiation induced precipitation in tungsten based, W-Re alloys', *Metall. Trans. A*, **April 1983**, **14A**, 655–666.
42. J. M. Steichen: 'Tensile properties of neutron irradiated TZM and tungsten', *J. Nucl. Mater.*, **Apr. 1976**, **60**, 13–19.
43. G. Janeschitz, K. Borrass, G. Federici, Y. Igithkanov, A. Kukushkin, H. D. Pacher, G. W. Pacher, and M. Sugihara: 'The ITER divertor concept', *J. Nucl. Mater.*, **Apr. 1995**, **220–222**, 73–88.
44. A. Gibson: 'Deuterium-tritium plasmas in the Joint European Torus (JET): behavior and implications', *Phys. Plasmas*, **May 1998**, **5**, 1839.
45. T. Tanno, A. Hasegawa, J.-C. He, M. Fujiwara, S. Nogami, M. Satou, T. Shishido, and K. Abe: 'Effects of transmutation elements on neutron irradiation hardening of tungsten', *Mater. Trans.*, **2007**, **48**, (9), 2399–2402.
46. M. Fukuda, K. Yabuuchi, S. Nogami, A. Hasegawa, and T. Tanaka: 'Microstructural development of tungsten and tungsten-rhenium alloys due to neutron irradiation in HFIR', *J. Nucl. Mater.*, **Dec. 2014**, **455**, 460–463.
47. P. R. Okamoto and L. E. Rehn: 'Radiation-induced segregation in binary and ternary alloys', *J. Nucl. Mater.*, **Aug. 1979**, **83**, 2–23.
48. R. Herschitz and D. N. Seidman: 'An atomic resolution study of radiation-induced precipitation and solute segregation effects in a neutron-irradiated W-25 at.% Re alloy', *Acta Metall.*, **Aug. 1984**, **32**, 1155–1171.
49. Y. Nemoto, A. Hasegawa, M. Satou, and K. Abe: 'Microstructural development of neutron irradiated W-Re alloys', *J. Nucl. Mater.*, **Dec. 2000**, **283–287**, 1144–1147.
50. T. Tanno, A. Hasegawa, J. C. He, M. Fujiwara, M. Satou, S. Nogami, K. Abe, and T. Shishido: 'Effects of transmutation elements on the microstructural evolution and electrical resistivity of neutron-irradiated tungsten', *J. Nucl. Mater.*, **Apr. 2009**, **386–388**, 218–221.
51. T. Tanno, M. Fukuda, S. Nogami, and A. Hasegawa: 'Microstructure development in neutron irradiated tungsten alloys', *Mater. Trans.*, **Jun. 2011**, **52**, 1447–1451.
52. M. Fukuda, T. Tanno, S. Nogami, and A. Hasegawa: 'Effects of Re content and fabrication process on microstructural changes and hardening in neutron irradiated tungsten', *Mater. Trans.*, **Nov. 2012**, **53**, 2145–2150.
53. L. Greenwood and F. Garner: 'Transmutation of Mo, Re, W, Hf, and V in various irradiation test facilities and STARFIRE', *J. Nucl. Mater.*, **September 1994**, **212–215**, 635–639.
54. L. R. Greenwood and F. A. Garner: 'Impact of transmutation issues on interpretation of data obtained from fast reactor irradiation experiments', *J. Nucl. Mater.*, **Aug. 2004**, **329–333**, 1147–1150.
55. J. He, G. Tang, A. Hasegawa, and K. Abe: 'Microstructural development and irradiation hardening of W and W-(3–26) wt%Re alloys after high-temperature neutron irradiation to 0.15 dpa', *Nucl. Fusion*, **Nov. 2006**, **46**, 877–883.
56. A. Hasegawa, M. Fukuda, T. Tanno, and S. Nogami: 'Neutron irradiation behavior of tungsten', *Mater. Trans.*, **Mar. 2013**, **54**, 466–471.
57. A. Hasegawa, T. Tanno, S. Nogami, and M. Satou: 'Property change mechanism in tungsten under neutron irradiation in various reactors', *J. Nucl. Mater.*, **Oct. 2011**, **417**, 491–494.
58. R. Nelson, D. Mazey, and J. Hudson: 'The use of ion accelerators to simulate fast neutron-induced voidage in metals', *J. Nucl. Mater.*, **Oct. 1970**, **37**, 1–12.
59. M. Toloczko, F. Garner, V. Voyevodin, V. Bryk, O. Borodin, V. Mel'nychenko, and A. Kalchenko: 'Ion-induced swelling of ODS ferritic alloy MA957 tubing to 500 dpa', *J. Nucl. Mater.*, **Oct. 2014**, **453**, 323–333.
60. G. S. Was: 'Fundamentals of radiation materials science: metals and alloys', **2007**, Berlin, Springer Science & Business Media.
61. J. T. Buswell: 'Vacancy damage in heavy ion and neutron-irradiated tungsten', *Philos. Mag.*, **Aug. 1970**, **22**, 787–802.
62. B. L. Eyre and R. Bullough: 'On the formation of interstitial loops in b.c.c. metals', *Philos. Mag.*, **Jul. 1965**, **12**, 31–39.
63. W. Jäger and M. Wilkens: 'Formation of vacancy-type dislocation loops in tungsten bombarded by 60 keV Au ions', *Phys. Status Solidi (a)*, **1975**, **32**, (1), 89–100.
64. F. Häussermann, M. Rühle, and M. Wilkens: 'Black-white contrast figures from small dislocation loops II. Application of the first order solution to small loops in ion-irradiated tungsten foils', *Phys. Status Solidi (b)*, **Apr. 1972**, **50**, 445–457.
65. A. Xu, C. Beck, D. E. J. Armstrong, K. Rajan, G. D. W. Smith, P. A. J. Bagot, and S. G. Roberts: 'Ion-irradiation-induced clustering in W-Re and W-Re-Os alloys: a comparative study using atom probe tomography and nanoindentation measurements', *Acta Mater.*, **Apr. 2015**, **87**, 121–127.
66. D. E. J. Armstrong, X. Yi, E. A. Marquis, and S. G. Roberts: 'Hardening of self ion implanted tungsten and tungsten 5-wt% rhenium', *J. Nucl. Mater.*, **Jan. 2013**, **432**, 428–436.
67. C. D. Hardie, S. G. Roberts, and A. J. Bushby: 'Understanding the effects of ion irradiation using nanoindentation techniques', *J. Nucl. Mater.*, **Dec. 2014**, **462**, 391–401.
68. D. E. J. Armstrong, A. J. Wilkinson, and S. G. Roberts: 'Mechanical properties of ion-implanted tungsten-5 wt% tantalum', *Phys. Scr.*, **Dec. 2011**, **T145**, 014076.
69. J. Gibson, D. Armstrong, and S. Roberts: 'The micro-mechanical properties of ion irradiated tungsten', *Phys. Scr.*, **Apr. 2014**, **T159**, 014056.
70. W. D. Nix and H. Gao: 'Indentation size effects in crystalline materials: a law for strain gradient plasticity', *J. Mech. Phys. Solids*, **Mar. 1998**, **46**, 411–425.
71. P. Hosemann, D. Kiener, Y. Wang, and S. A. Maloy: 'Issues to consider using nano indentation on shallow ion beam irradiated materials', *Journal of Nuclear Materials*, **Jun. 2012**, **425**, 136–139.
72. M. J. Baldwin and R. P. Doerner: 'Formation of helium induced nanostructure 'fuzz' on various tungsten grades', *J. Nucl. Mater.*, **Sep. 2010**, **404**, 165–173.
73. C. S. Becquart and C. Domain: 'A density functional theory assessment of the clustering behaviour of He and H in tungsten', *J. Nucl. Mater.*, **Apr. 2009**, **386–388**, 109–111.
74. S. Takamura, N. Ohno, D. Nishijima, and S. Kajita: 'Formation of nanostructured tungsten with arborescent shape due to helium plasma irradiation', *Plasma Fusion Res.*, **Dec. 2006**, **1**, 051–051.
75. T. J. Petty, M. J. Baldwin, M. I. Hasan, R. P. Doerner, and J. W. Bradley: 'Tungsten 'fuzz' growth re-examined: the dependence on ion fluence in non-erosive and erosive helium plasma', *Nucl. Fusion*, **Sep. 2015**, **55**, 093033.
76. M. Miyamoto, T. Watanabe, H. Nagashima, D. Nishijima, R. P. Doerner, S. I. Krashennnikov, A. Sagara, and N. Yoshida: 'In situ transmission electron microscope observation of the formation of fuzzy structures on tungsten', *Phys. Scr.*, **Apr. 2014**, **T159**, 014028.
77. F. Sefta, K. D. Hammond, N. Juslin, and B. D. Wirth: 'Tungsten surface evolution by helium bubble nucleation, growth and rupture', *Nucl. Fusion*, **Jul. 2013**, **53**, 073015.
78. D. Nishijima, M. J. Baldwin, R. P. Doerner, and J. H. Yu: 'Sputtering properties of tungsten 'fuzzy' surfaces', *J. Nucl. Mater.*, **Aug. 2011**, **415**, S96–S99.
79. F. Hofmann, D. Nguyen-Manh, M. R. Gilbert, C. E. Beck, J. K. Eliason, A. A. Maznev, W. Liu, D. E. J. Armstrong, K. A. Nelson, and S. L. Dudarev: 'Lattice swelling and modulus change in a helium-implanted tungsten alloy: X-ray micro-diffraction, surface acoustic wave measurements, and multiscale modelling', *Acta Mater.*, **May 2015**, **89**, 352–363.
80. D. E. J. Armstrong, P. D. Edmondson, and S. G. Roberts: 'Effects of sequential tungsten and helium ion implantation on nano-indentation hardness of tungsten', *Appl. Phys. Lett.*, **2013**, **102**, (25), 251901.
81. J. S. K. Gibson: 'Fusion power (PhD thesis, small)', PhD thesis, 2015, Oxford, University of Oxford.
82. S. Zinkle and N. Ghoniem: 'Operating temperature windows for fusion reactor structural materials', *Fusion Eng. Design*, **Nov. 2000**, **51–52**, 55–71.
83. A. Giannattasio, Z. Yao, E. Tarleton, and S. G. Roberts: 'Brittle-ductile transitions in polycrystalline tungsten', *Philos. Mag.*, **2010**, **90**, (30), 3947–3959.
84. E. Tarleton and S. Roberts: 'Dislocation dynamic modelling of the brittle-ductile transition in tungsten', *Philos. Mag.*, **November 2009**, **89**, (31), 2759–2769.
85. C. D. Hardie and S. G. Roberts: 'Nanoindentation of model Fe-Cr alloys with self-ion irradiation', *J. Nucl. Mater.*, **Feb. 2013**, **433**, 174–179.
86. J.-C. He, A. Hasegawa, M. Fujiwara, M. Satou, T. Shishido, and K. Abe: 'Fabrication and characterization of W-Re-Os alloys for studying transmutation effects of W in fusion reactors', *Mater. Trans.*, **Jun. 2004**, **45**, 2657–2660.
87. M. R. Gilbert, J. Marian, and J.-C. Sublet: 'Energy spectra of primary knock-on atoms under neutron irradiation', *J. Nucl. Mater.*, **Dec. 2015**, **467**, 121–134.